Monatshefte für Chemie 132, 1527–1546 (2001)

Monatshefte für Chemie
Chemical Monthly

Fluorophenyl Bilirubins: Synthesis and Stereochemistry

Justin O. Brower and **David A. Lightner***

Department of Chemistry, University of Nevada, Reno, NV 89557-0020, USA

Summary. Analogs of bilirubin with vinyl groups replaced by symmetrically-disposed *o*-fluorophenyls (**1**, *bis-exo*, and **2**, *bis-endo*) were synthesized and characterized spectroscopically. Their ^{1}H NMR spectra and NOE data are consistent with an intramolecularly hydrogen-bonded ridge-tile conformation where each propionic acid group embraces an opposing dipyrrinone. Like bilirubin, **1** and **2** exhibit negative chirality induced circular dichroism (ICD) *Cotton* effects in chloroform containing quinine. Unlike bilirubin, however, in aqueous buffer containing human serum albumin, **2** exhibits a negative exciton chirality ICD, whereas that of **1** is positive.

Keywords. Pyrroles; Conformation; Hydrogen-bonding; Circular dichroism.

Introduction

Bilirubin-IXα (Fig. 1A), the yellow pigment of jaundice, is an important and structurally intriguing mammalian natural product produced copiously in normal human metabolism from hemoglobin and other heme proteins [1, 2]. Studies aiming at understanding its properties and relating them to its metabolism have focussed on the pigment's unique ability to fold into a conformation where its carboxylic acids engage in hydrogen bonding to the opposing dipyrrinones (Fig. 1B) [3, 4]. Dipyrrinones are known to hydrogen bond very strongly to carboxylic acids [5–8], and in bilirubin such hydrogen bonding profoundly decreases its polarity. This makes bilirubin too lipophilic to be excreted in normal metabolism and thus requires hepatic glucuronidation for elimination into bile [2, 9]. Analogs of bilirubin with vinyl groups located symmetrically, such as bilirubin-IIIα and XIIIα (**3** and **4**, Fig. 1C) exhibit solution and metabolism properties that are very nearly the same as those of bilirubin. However, analogs with propionic acids displaced from their natural locations at C(8) and C(12) cannot engage in conformation stabilizing intramolecular hydrogen bonding, which makes them very polar and thus differently behaved in solution and metabolism from bilirubin [10]. In order to determine whether the properties and even the metabolism of bilirubin are significantly changed by replacing vinyl groups with aromatic rings (as when vinyls are replaced with *n*-butyls [11]), we synthesized **1** and **2** (Fig. 1C), two new symmetric bilirubins with *o*-fluorophenyl groups replacing the vinyls of

* Corresponding author. E-mail: lightner@unr.edu

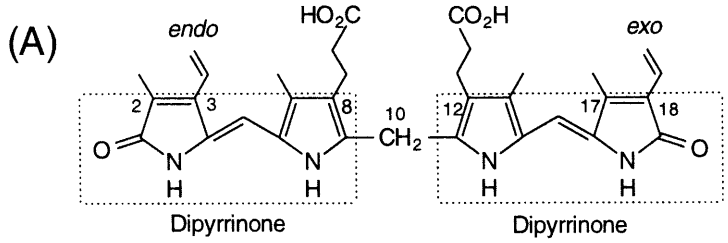

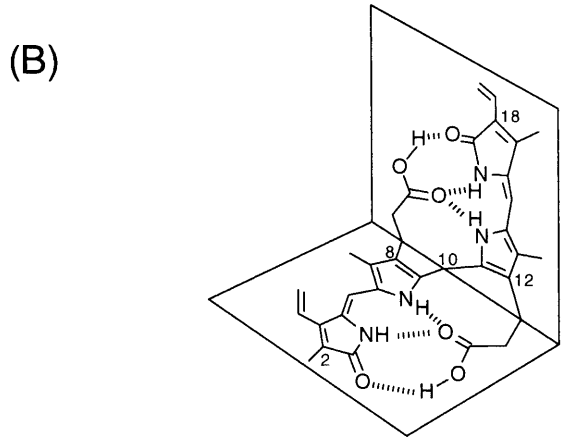

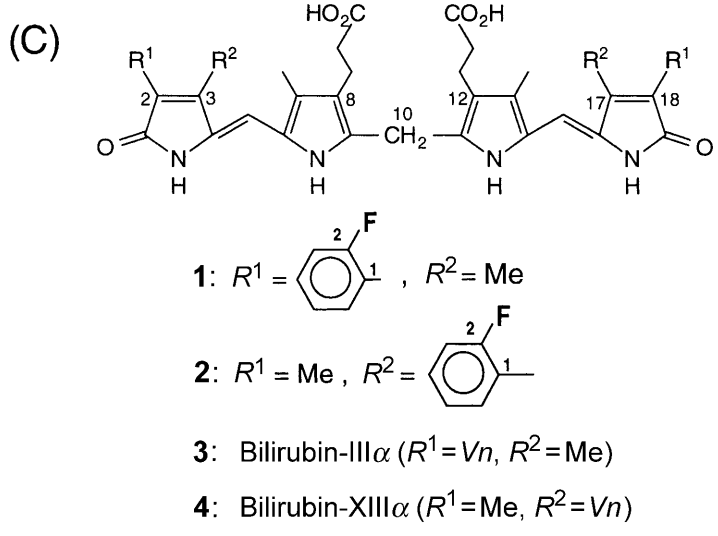

Fig. 1. **(A)** Bilirubin-IXα (bilirubin), shown with its two dipyrrinone chromophores arranged in a linear shape, is nonsymmetric; **(B)** bilirubin in its energetically most stable, intramolecularly hydrogen-bonded ridge-tile conformation; only one of two enantiomeric conformers is shown, and hydrogen bonds are indicated by hatched lines; **(C)** linear representations for two new symmetric *o*-fluorophenyl rubins **1** and **2** and their symmetric bilirubin analogs (**3** and **4**)

mesobilirubin-IIIα (**3**) and -XIIIα (**4**). We chose the *o*-fluorophenyl group because of our interest in preparing bilirubin analogs possessing an MRI sensitive fluorine label. In this paper, we describe the synthesis, stereochemistry, and solution properties of these novel bilirubins.

Results and Discussion

Synthesis aspects

Since *o*-fluorophenyl rubins **1** and **2** share a common dipyrrylmethane central core, the known dipyrrylmethane dialdehyde **16** [12] became the key synthetic intermediate to be coupled with either pyrrolinone **7** or **8** (Scheme 1). Pyrrolinones **7** and **8** were prepared in a standard series of steps using *Barton-Zard* pyrrole-forming reactions [11, 13]. Thus, reaction of 2-nitro-1-(2-fluorophenyl)-ethyl acetate (**15**) with *p*-toluenesulfonyl isocyanide (*TosMIC*) gave one (**12**) of the two required monopyrrole precursors in 54% yield. Nitro acetate **15** was prepared by standard acetylation methods from the corresponding nitro alcohol, which was prepared by a *Henry* reaction between 1-nitroethane and 2-fluorobenzaldehyde using KF as base. A similar direct route to the monopyrrole (**11**) necessitated the synthesis of the isomeric 1-nitro-2-(2-fluorophenyl)-ethyl acetate, which in turn requires the less available 2-fluoro-α-nitrotoluene as starting material. Consequently, we decided to convert **12** into **11** by means of an acid-catalyzed isomerization described earlier for converting the phenyl analog of **12** to the phenyl analog of **11** [14]. We found that **12** was smoothly isomerized to **11** in 95% isolated yield catalyzed by trifluoroacetic acid (*TFA*) in dichloromethane. Tosyl pyrroles **11** and **12** were converted independently to pyrrolinones **9** and **10**, respectively, in the conventional way [11]. Thus, bromination of **11** with phenyltrimethylammonium tribromide gave **13** in 97% yield, whereas the same reagents and conditions converted **12** to **14** in 87% yield. Treatment of **13** with *TFA* and water gave tosylpyrrolinone **9** in 86% yield, and similar treatment of **14** afforded **10** in 99% yield. The tosyl groups of **9** and **10** were removed by reduction with sodium borohydride in ethanol, affording **7** and **8**, respectively, in 98% and 90% isolated yields.

The final, bilirubin-forming coupling steps involved the reaction of dipyrrole dialdehyde **16** [12] with excess **7** in refluxing aqueous methanolic KOH and afforded **1** as a bright yellow solid in 59% yield. The similar reaction of **16** with **8** proceeded less well and gave **2** in only 27% isolated yield. Presumably, the location of the *o*-fluorophenyl group on **8** sterically shields the adjacent reaction center, thus slowing down the base-catalyzed condensation.

Solution properties

The bilirubin with *o*-fluorophenyl groups replacing the *exo* vinyls of **3** was found to give only slightly longer HPLC retention times using a reverse phase column (**1**: 16.7 min, **3**: 16.4 min). In contrast, substituting *o*-fluorophenyl groups for *endo* vinyls of **4** produced significantly shorter retention times (**2**: 12.9 min, **4**: 14.5 min). These data suggest that whereas **1** and **3** might have similar polarities, **2** would be noticeably more polar than **4** (and **1**). Confirmation comes from TLC on silica gel using 1% CH_3OH in CH_2Cl_2 as eluent: **1** ($R_f = 0.67$) moved faster than **2**

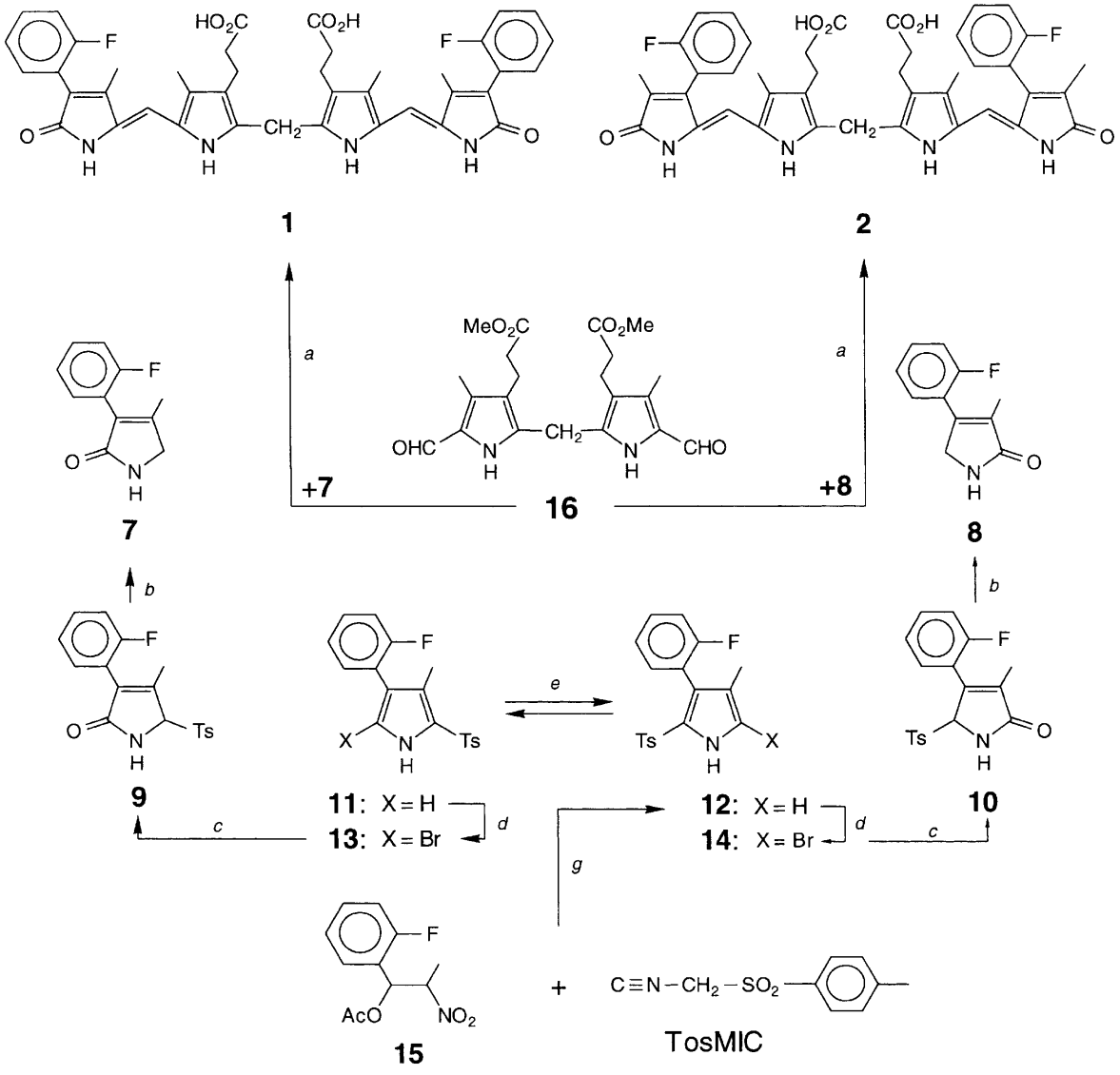

Scheme 1. Reagents and conditions: [a]KOH/CH_3OH-H_2O/refl., then HCl; [b]$NaBH_4$/EtOH; [c]*TFA*-H_2O (5:1); [d]$PhNBMe_3^+Br_3^-/CH_2Cl_2$; [e]*TFA*/$CH_2Cl_2$; [g]$K_2CO_3$/*THF*-*i*PrOH

($R_f = 0.55$), **4** ($R_f = 0.53$), and **3** ($R_f = 0.53$), which had nearly identical R_f values as **3** and **4**. The data suggest that the presence of the large aromatic group at the *exo* position of the lactam rings shields the polar lactam group from the silica surface more effectively than an *exo* methyl group.

^{13}C NMR spectroscopy and structure

The constitutional structures of bilirubins-IIIα and -XIIIα (**3** and **4**) are well-established [1, 15], and the structures of **1** and **3** differ only in the *exo* substituents (*o*-fluorophenyl in **1**, vinyl in **3**), whereas the structures of **2** and **4** differ similarly

Table 1. Comparison of ^{13}C NMR chemical shift assignments for *o*-fluorophenyl mesobilirubin analogs **1** ($R^1 =$ 2-F-Ph, $R^2 =$ Me) and **2** ($R^1 =$ Me, $R^2 =$ 2-F-Ph) with mesobilirubin-IIIα ($R^1 =$ *Vn*, $R^2 =$ Me; **3**) and mesobilirubin-XIII α ($R^1 =$ Me, $R^2 =$ *Vn*; **4**) in $(CD_3)_2SO$[a]

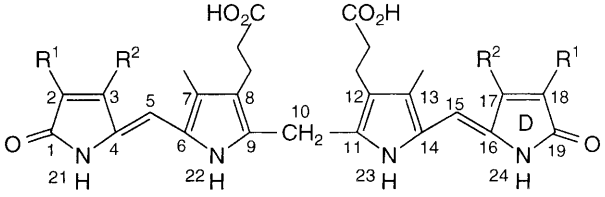

Position	**1**	**2**	**3**	**4**
1,19-CO	169.47	170.78	170.38	171.31
2,18	122.05	126.16	122.38	123.42
2,18-CH_3 or 3,17-CH_3	10.88	8.99	9.25	9.47
3^1,17^1 (or 2^1,18^1)	119.92	119.48	–	–
3^2,17^2 (or 2^2,18^2)	159.40	159.18	–	–
3^3,17^3 (or 2^3,18^3)	115.59	116.03	–	–
3^4,17^4 (or 2^4,18^4)	124.08	124.51	–	–
3^5,17^5 (or 2^5,18^5)	129.82	131.03	–	–
3^6,17^6 (or 2^6,18^6)	132.11	131.81	–	–
3,17	144.52	139.15	141.96	140.36
4,16	128.41	127.51	128.21	127.43
5,15-CH=	100.35	100.71	100.00	99.13
6,14	121.81	121.90	122.23	122.04
7,13	119.87	119.64	119.79	119.52
7,13-CH_3	9.18	9.28	9.13	9.12
8,12	124.36	123.46	124.11	123.21
8^1,12^1-CH_2	19.26	19.16	19.21	19.22
8^2,12^2-CH_2	34.19	34.18	34.17	34.21
8^3,12^3-COOH	173.99	173.91	173.91	173.93
9,11	131.45	131.03	131.34	130.79
10-CH_2	23.78	23.61	23.67	23.58

[a] Chemical shifts in δ (ppm) downfield from *TMS*

and only in the nature of the *endo* substituents. Consequently, it is not surprising that the ^{13}C NMR spectroscopic data (Table 1) for **1** and **2** are rather similar to those of **3** and **4**. Carbons bearing the altered substituents can be expected to exhibit the largest chemical shift differences; however, ring carbons 2 and 18 of **1** and **3** exhibit only slight differences, whereas the methyl-bearing ring carbons 3 and 17 are by about 2.5 ppm more deshielded in **1** than in **3**. Similarly, the methyl-bearing ring carbons 2 and 18 of **2** are more deshielded than those of **4** by *ca.* 2.5 ppm, but ring carbons 3 and 17 are $\sim$1 ppm more shielded in **2** relative to **4**. Ring carbons 4/16, 6/4, 7/13, 8/12, and 9/11 of **1** and **3** and **2** and **4** do not show a similar sensitivity; nor do bridging carbons 5/15 and 10. The chemical shifts of the methyl groups at 2/18 and 3/17 are more shielded in **1** than in **3**, but in **2** they are more deshielded than in **4**. The chemical shift differences observed between **1** and **2** are found in parallel to those of **3** and **4**.

Analysis of hydrogen bonding and conformation by ^1H NMR

Bilirubin and its symmetric analogs **3** and **4** are each composed of two dipyrrinones (Fig. 1) which are known to participate in tight carboxylic acid to dipyrrinone intramolecular hydrogen bonding [3, 4, 6, 16, 17]. Such hydrogen bonding strongly deshields the dipyrrinone lactam and pyrrole NH (~7.5 and 8 ppm, respectively, in the monomers [5]), causing large deshieldings in $CDCl_3$. Similarly large

Table 2. ^{1}H NMR chemical shift assignments for bilirubin analogs **1** (R^1 = 2-F-Ph, R^2 = Me) and **2** (R^1 = Me, R^2 = 2-F-Ph) with **3** (R^1 = *Vn*, R^2 = Me) and **4** (R^1 = Me, R^2 = *Vn*) in $(CD_3)_2SO$[a] and $CDCl_3$[a,b]

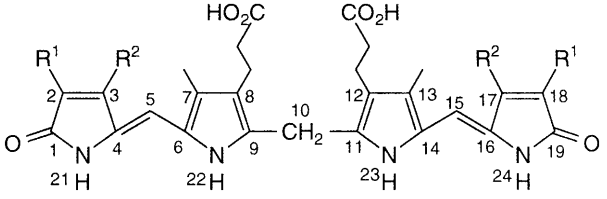

Position	**1**	**2**	**3**	**4**
α,α'-COOH	11.93	11.87	11.89	11.89
	13.53	*13.60*	*13.71*	*13.67*
21,24-NHCO	10.13	10.32	9.90	10.03
	10.88	*10.98*	*10.70*	*10.79*
22,23-NH	10.55	10.49	10.49	10.43
	9.36	*9.25*	*9.30*	*9.26*
2,18 (or 3,17)-CH_3	2.11	1.74	2.16	2.00
	2.14	*1.86*	*2.18*	*2.16*
3^3,17^3 (or 2^3,18^3)-ArH	7.40	7.39	–	–
	7.31	*7.42*	–	–
3^4,17^4 (or 2^4,18^4)-ArH	7.29	7.38	–	–
	7.37	*7.43*	–	–
3^5,17^5 (or 2^5,18^5)-ArH	7.43	7.55	–	–
	7.19	*7.23*	–	–
3^6,17^6 (or 2^6,18^6)-ArH	7.27	7.37	–	–
	7.12	*7.21*	–	–
5,15-CH=	6.19	5.57	6.09	6.09
	6.26	*5.84*	*6.21*	*6.14*
7,13-CH_3	2.06	1.77	2.13	1.92
	2.20	*2.02*	*2.15*	*1.99*
8^1,12^1-CH_2	2.45[c]	2.39[c]	2.42[e]	2.42[f]
	3.04[d]	*3.01*[d]	*3.01*[d]	*3.02*[d]
	2.60[d]	*2.56*[d]	*2.58*[d]	*2.58*[d]
8^2,12^2-CH_2	1.96[c]	1.93[c]	1.93[e]	1.94[f]
	2.92[d]	*2.89*[d]	*2.90*[d]	*2.90*[d]
	2.82[d]	*2.80*[d]	*2.81*[d]	*2.82*[d]
10-CH_2	4.03	3.98	4.00	3.98
	4.11	*4.08*	*4.08*	*4.08*

[a] Chemical shifts in δ (ppm) downfield from *TMS*; [b] values in italics are from $CDCl_3$.; [c] t, J = 7.8 Hz; [d] multiplets, see Table 3 for coupling constants; [e] t, J = 7.5 Hz; [f] t, J = 8.5 Hz

deshieldings are found in dipyrrinone–dipyrrinone intermolecularly hydrogen-bonded dimers in $CDCl_3$ [5, 6]. In bilirubins, the dipyrrinone NH chemical shifts have been used to detect and distinguish dipyrrinone to dipyrrinone intermolecular hydrogen bonding [5, 6, 8, 16] from dipyrrinone to carboxylic acid intramolecular hydrogen bonding [4, 6–8, 16–18]. Such ^1H NMR studies have shown that the pyrrole NH resonance of bilirubin in $CDCl_3$ is found at *ca.* 9.2 ppm when the dipyrrinone and carboxylic acid groups are linked by intramolecular hydrogen bonding, which is ~1 ppm upfield relative to the pyrrole NH chemical shift (~10.2 ppm) found for planar dipyrrinone to dipyrrinone dimers [5, 6, 8].

The data of Table 2 show chemical shift of *ca.* 9.3 ppm for the pyrrole NH in **1**–**4** in $CDCl_3$, which we believe to be consistent with dipyrrinone to carboxylic acid intramolecular hydrogen bonding of the type shown in Fig. 1B. In contrast, in $(CD_3)_2SO$, a solvent thought to insert into the bilirubin hydrogen bonding matrix [16–21], the CO_2H and lactam NH signals become more shielded than in $CDCl_3$, whereas the pyrrole NH typically becomes more deshielded.

The stereochemical conclusions reached above were confirmed by $^1H\{^1H\}$ homonuclear *Overhauser* effect (NOE) measurements in $CDCl_3$ (Fig. 2). Significantly, and consistent with a ridge-tile conformation (Fig. 1B), NOEs are observed between the carboxylic acid hydrogen and the lactam NH of **1**–**4**. The NOE measurements also confirm *syn-Z*-dipyrrinone conformation: moderately strong NOEs found between (*i*) the pyrrole and lactam NHs within individual dipyrrinones and (*ii*) the vinylic hydrogens at C(5) and C(15) and the pyrrole methyls at C(7) and C(13) and the lactam methyls at C(3) and C(17).

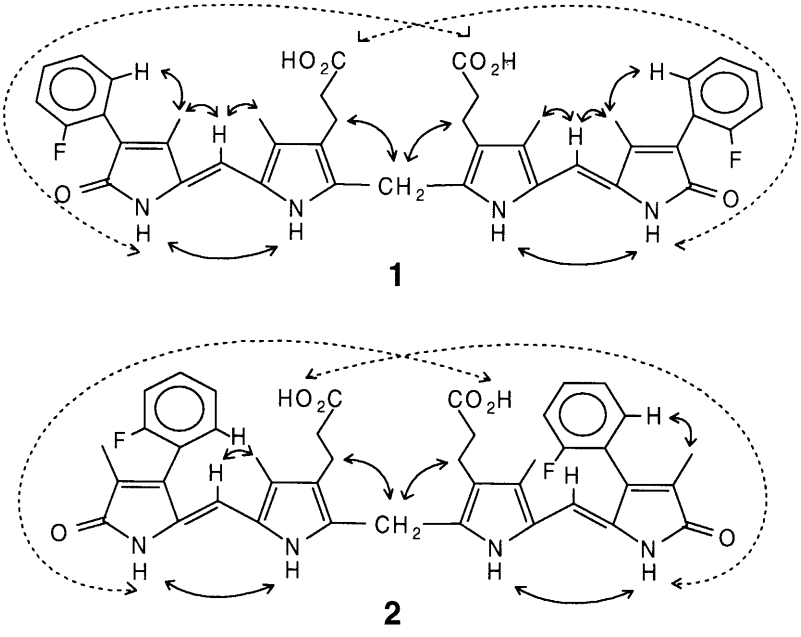

Fig. 2. $^1H\{^1H\}$ Homonuclear *Overhauser* effects (NOEs) found in **1** and **2** in $CDCl_3$ are shown by solid, double-headed curved arrows; significant, albeit weak, NOEs are found between the CO_2H protons and the lactam NH protons (indicated by dashed arrows)

Table 3. ^{1}H NMR chemical shifts[a] and coupling constants[b] for the propionic acid $-C_\beta H_A H_X-C_\alpha H_B H_C-CO_2H$ segments of **1**–**4** in $CDCl_3$ at 22°C

		β-CH_2				α-CH_2			
MBR		H_X		H_A		H_B		H_C	
1	δ:	2.60		3.04		2.92		2.82	
		J_{BX}	2.7	J_{AB}	13.8	J_{AB}	13.8	J_{AC}	2.1
		J_{CX}	3.2	J_{AC}	2.1	J_{BX}	2.7	J_{CX}	3.2
		J_{AX}	−13.2	J_{AX}	−13.2	J_{BC}	−18.5	J_{BC}	−18.5
2	δ:	2.56		3.01		2.89		2.80	
		J_{BX}	2.5	J_{AB}	13.7	J_{AB}	13.7	J_{AC}	2.7
		J_{CX}	3.1	J_{AC}	2.7	J_{BX}	2.5	J_{CX}	3.1
		J_{AX}	−14.0	J_{AX}	−14.0	J_{BC}	−16.0	J_{BC}	−16.0
3	δ:	2.58		3.01		2.90		2.81	
		J_{BX}	2.0	J_{AB}	14.5	J_{AB}	14.5	J_{AC}	2.5
		J_{CX}	3.5	J_{AC}	2.5	J_{BX}	2.0	J_{CX}	3.5
		J_{AX}	−13.5	J_{AX}	−13.5	J_{BC}	−17.0	J_{BC}	−17.0
4	δ:	2.58		3.02		2.90		2.82	
		J_{BX}	2.0	J_{AB}	14.0	J_{AB}	14.0	J_{AC}	2.5
		J_{CX}	4.0	J_{AC}	2.5	J_{BX}	2.0	J_{CX}	4.0
		J_{AX}	−14.0	J_{AX}	−14.0	J_{BC}	−18.5	J_{BC}	−18.5

[a] δ (ppm) downfield from *TMS*; [b] J in Hz from 500 MHz spectra

Further evidence for intramolecular hydrogen bonding between propionic acid and dipyrrinone groups in the bilirubins can be elicited from an examination of vicinal coupling constants (Table 3). In $CDCl_3$, the well-defined ABCX (ddd) coupling pattern is characteristic of restricted mobility [16, 17, 22, 23] in the $-CH_AH_XCH_BH_C-COOH$ segment which is constrained to adopt a fixed staggered geometry due to strong intramolecular hydrogen bonding. Analysis of $^3J_{HH}$ in the propionic acid chains clearly shows the ABCX pattern of the fixed staggered propionic acid geometry in **1**–**4**, thus providing strong supporting experimental evidence for folded ridge-tile structures. On the other hand, the less complicated A_2B_2 pattern found in $(CD_3)_2SO$ (Table 2) indicates more motional freedom in the propionic acid segment, whose CO_2H groups are thought to be linked to the dipyrrinones *via* bound solvent molecules [17, 19, 21, 22]. Taken collectively, the NMR data support intramolecularly hydrogen-bonded ridge-tiles for **1**–**4** (Figure 3) and a fixed staggered conformation of the propionic acid segments.

UV/Vis spectroscopic analysis

The UV/Vis spectra of **1**–**4** in a wide range of solvents of different polarity and hydrogen bonding ability are rather similar (Table 4). In polar solvents, **1**–**4** invariably show $\lambda^{max} \approx 440$–$450$ nm and a shoulder near 430 nm. In nonpolar solvents, λ^{max} lies at about 450–460 nm, with a shoulder near 430–440 nm. The band shape is due to two exciton components originating in an electric transition

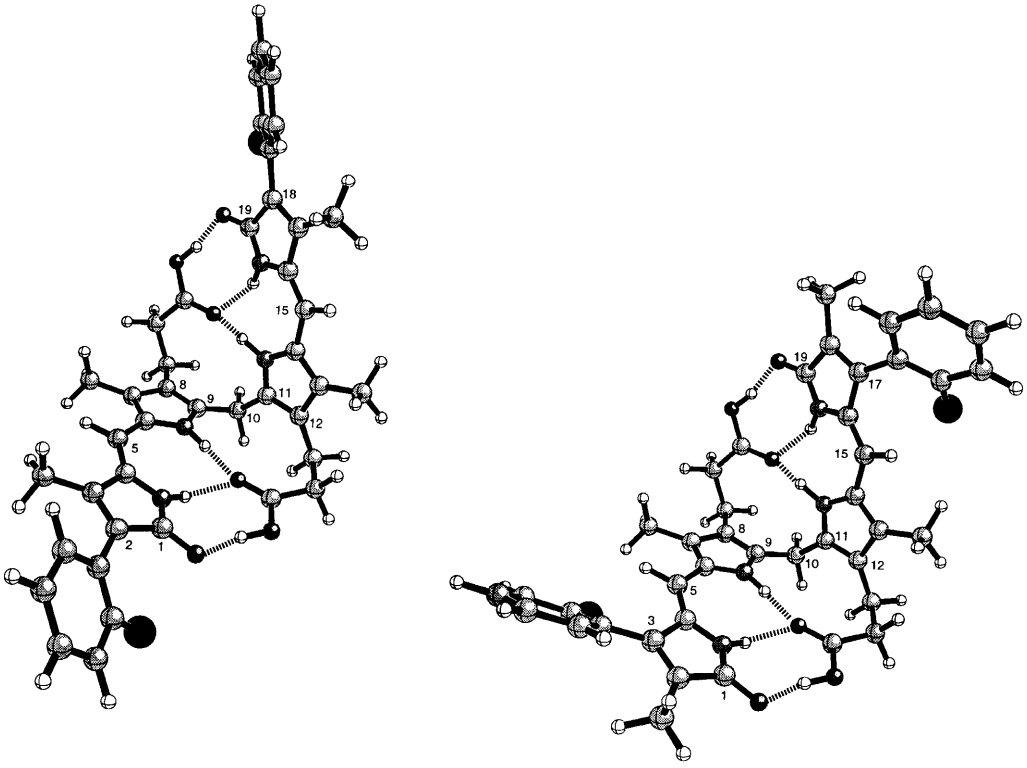

Fig. 3. Ball and Stick [20] representations of the Sybyl molecular dynamics energy-minimized conformations of *o*-fluorophenyl rubins **1** (left) and **2** (right) illustrating the greater proximity of the *exo o*-fluorophenyl group of **1** to its lactam carbonyl hydrogen bonding region; hatched lines represent hydrogen bonds

dipole–dipole interaction between the two proximal dipyrrinone chromophores oriented at an angle of 90° (as in Fig. 4) [4]. The data are consistent with the ridge-tile conformation for **1**–**4** derived from NMR studies and support the conformational analysis by circular dichroism spectroscopy given below.

Induced circular dichroism and conformation

Stereochemical investigations of bilirubin and its analogs have repeatedly indicated that (*i*) the most stable conformation is one where the two dipyrrinones are rotated into a ridge-tile shape, (*ii*) considerable stabilization of the ridge-tile is achieved by intramolecular hydrogen bonding, and (*iii*) the pigment adopts either of two interconverting enantiomeric ridge-tiles as depicted in Fig. 3 [4, 17, 23, 24]. The component dipyrrinone chromophores of **1**–**4** have strongly-allowed long-wavelength electronic transitions (Table 4), making them excellent candidates for transition dipole–dipole interaction (exciton coupling) [24, 25] (Fig. 4). Such intramolecular exciton interaction or resonance splitting produces two long wavelength transitions in the UV/Vis spectrum and two corresponding but oppositely-signed bands in the CD spectrum. According to exciton chirality theory [26], a long-wavelength negative and short-wavelength positive CD couplet exhibits

Table 4. Solvent dependence of UV/Vis spectroscopic data of rubins **1–4**[a]

Rubin	ε^{max} (λ^{max}/nm)					
	Benzene	$CHCl_3$	$(CH_3)_2CO$	CH_3OH	CH_3CN	$(CH_3)_2SO$
	62000 (458)	61000 (456)	60400 (452)	59800 (449)	61400 (449)	61600 (452)
1	57000 (444)^{sh}	58300 (444)^{sh}	56000 (436)^{sh}	52300 (428)^{sh}	57000 (434)^{sh}	50800 (421)^{sh}
	58000 (451)	57400 (449)	56600 (445)	55700 (442)	56500 (442)	60100 (444)
2	53000 (435)^{sh}	55000 (437)^{sh}	52400 (429)^{sh}	48700 (421)^{sh}	52700 (426)^{sh}	47800 (413)^{sh}
	61690 (460)	64610 (456)	62360 (451)	60700 (451)	62360 (451)	67760 (459)
3	48070 (426)^{sh}	49560 (424)^{sh}	50890 (424)^{sh}	49120 (417)^{sh}	51220 (423)^{sh}	48810 (416)^{sh}
			46580 (447)	45310 (446)	46980 (445)	47830 (446)
4	45580 (447)	46920 (450)	34610 (415)^{sh}	37540 (416)^{sh}	39430 (417)^{sh}	37670 (415)^{sh}

[a] 22°C, $\sim 1.4 \times 10^{-5} M$; [sh] shoulders or inflections were determined by first and second derivative spectra

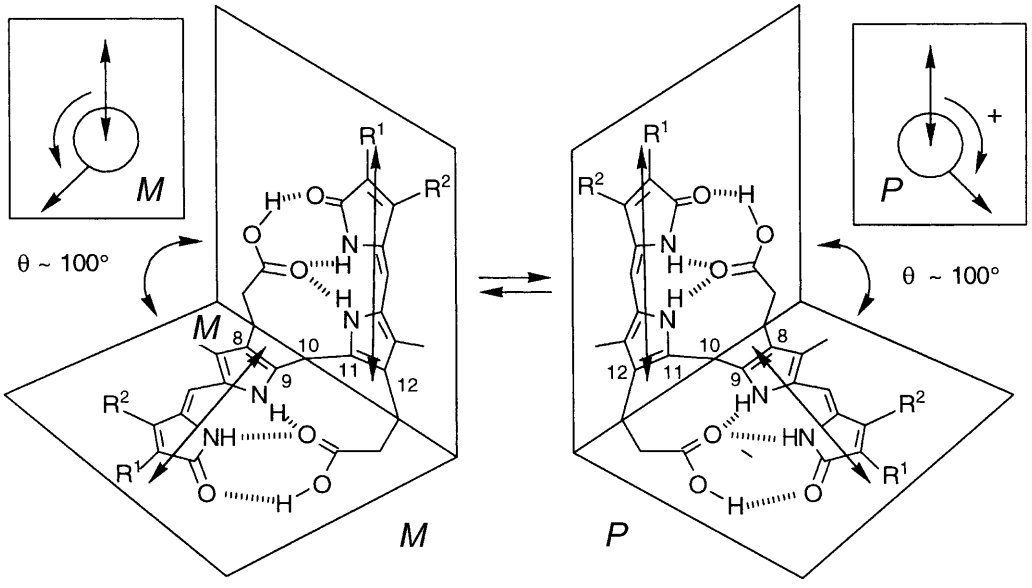

Fig. 4. Interconverting intramolecularly hydrogen-bonded enantiomeric conformers of bilirubins **1–4** (see Fig. 1 for R^1, R^2); the double headed arrows represent the dipyrrinone long-wavelength electric transition moments (dipoles); the relative helicities (*M*, minus or *P*, plus) of the dipole vectors are shown (inset) for each enantiomer; hydrogen bonds are indicated by hatched lines

negative exciton chirality and corresponds to a negative helical disposition of the relevant dipyrrinone long-wavelength transition dipoles. Usually, this corresponds to the *M*-helical enantiomeric type of Fig. 4 [4, 24].

In a nonpolar, aprotic solvent such as chloroform, the conformational equilibrium between bilirubin enantiomers can be displaced from 1:1 by adding a chiral recognition agent [11, 24]. This leads typically to an intense bisignate induced circular dichroism (ICD) *Cotton* effect, as has been noted previously for bilirubin in aqueous buffers with added albumin [11, 27] and in chloroform

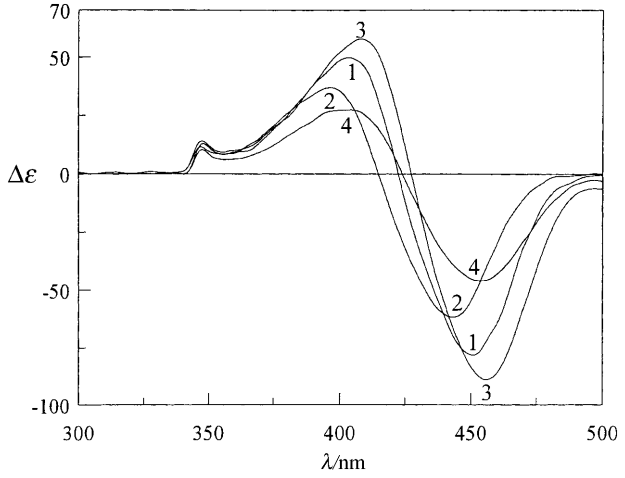

Fig. 5. Circular dichroism spectra of $1.4 \times 10^{-5}\,M$ **1–4** in $CHCl_3$ in the presence of *ca.* $4.2 \times 10^{-3}\,M$ quinine at 22°C; the compound's number is indicated on each CD curve

with added quinine [11, 24] or other optically active amines [28]. Similarly, for the bilirubins discussed here, in $CHCl_3$ strong negative exciton chirality ICDs are observed in the presence of quinine (Fig. 5), as is characteristic of an exciton system in which the two dipyrrinone chromophores of the bichromophoric rubin molecule interact by coupling locally excited $\pi \rightarrow \pi^*$ transitions (electric dipole transition moment coupling). At a molar ratio of quinine:pigment $\approx 300:1$, the *Cotton* effect intensities reach a maximum for **3**, giving an intense bisignate CD ($\Delta\varepsilon_{456}^{max} = -89, \Delta\varepsilon_{408}^{max} = +58$) of exactly the same signed order but larger magnitudes than those seen for bilirubin or **4** [24]. The *Cotton* effect intensities of **1** are nearly identical to those of its counterpart **3**, whereas those of **2** are very similar; only **4** exhibits smaller magnitudes. Interestingly, the presence of the larger unsaturated group (*o*-fluorophenyl or vinyl) in the *exo* positions leads to more intense *Cotton* effects (**1** and **3**) than when they are located at the *endo* sites (**2** and **4**; Table 5). Whether this reflects ineffective complexation/recognition or an altered pigment conformation is not immediately clear, but the presence of the unsaturated

Table 5. Comparison of circular dichroism and UV/Vis spectroscopic data for **1–4** in $CHCl_3$ solutions containing quinine[a]

Pigment	CD			UV/Vis	
	$\Delta\varepsilon^{max}$ $(\lambda)_1$	λ_2 at $\Delta\varepsilon = 0$	$\Delta\varepsilon^{max}$ $(\lambda)_3$	ε^{max}	λ(nm)
1	+52 (403)	422	−82 (452)	54910	456
2	+46 (403)	419	−80 (446)	57140	448
3	+58 (408)	427	−89 (456)	63330	458
4	+39 (405)	425	−64 (453)	56790	455

[a] Pigment conc.: $\sim 1.4 \times 10^{-5}\,M$; quinine conc.: $\sim 4.2 \times 10^{-3}\,M$; pigment:quinine molar ratio = ~1:300

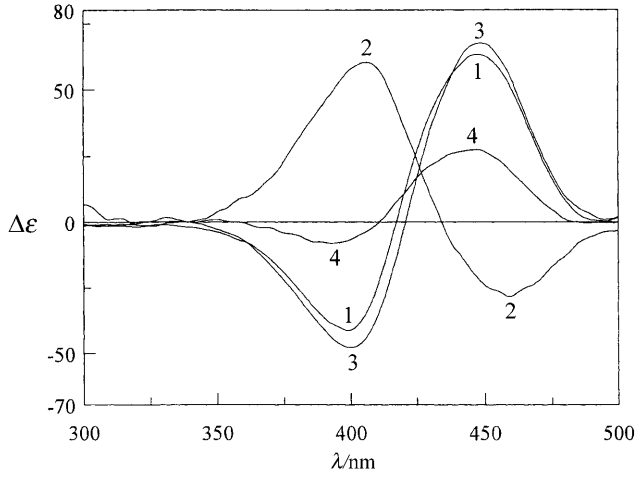

Fig. 6. Circular dichroism spectra of 1.41×10^{-5} *M* **1**–**4** in the presence of *ca.* 2.8×10^{-5} *M* HSA in *pH* 7.4 *Tris* buffer at 22°C; the compound's number is indicated on each CD curve

substituent nearer the lactam carbonyl leads to larger ICDs and perhaps promotes stronger complexation with quinine.

When human serum albumin (HSA) is used as the chiral complexation agent, aqueous buffered ($pH = 7.4$, *Tris*) solutions of **1**, **3**, and **4** exhibit strong positive chirality bisignate ICD *Cotton* effects as observed for bilirubin [27]. In contrast, **2** exhibits a strong negative bisignate ICD *Cotton* effect (Fig. 6). The CD intensities of **1** are similar to those of **3**, and both are more than twice as large as those of **4**. The data suggest a greater enantioselective chiral complexation by HSA for **1** and **3** than **4** and implicate the larger *exo* groups to produce a favorable binding interaction with the chiral complexation agent. The data are qualitatively similar to those seen with the corresponding mesobilirubins-IIIα and -XIIIα (vinyls reduced to ethyls) and their *n*-methyl analogs [11]. The ICD data for **1**, **3**, and **4** suggest rather similar conformations on HSA, whereas the contrasting ICD data for **2** suggest a mirror image or different conformation.

Adding 5 mm^3 of $CHCl_3$ to 5 cm^3 of a *pH* 7.4 buffered aqueous HSA solution of **2** leads to a very striking intensification of its *Cotton* effect (Fig. 7). Addition of a second 5 mm^3 aliquot effects essentially no change. In contrast, and as noted previously for bilirubin [29], addition of 5 mm^3 of $CHCl_3$ to *pH* 7.4 aqueous buffered HSA solutions of **1** and **4** leads to *Cotton* effect sign inversions (Figs. 8 and 9). The *Cotton* effect magnitudes increase in intensity upon addition of a second 5 mm^3 aliquot of $CHCl_3$, but not strongly. Although the first 5 mm^3 of $CHCl_3$ do not invert the CD of **3** (Fig. 10), the second do. At a total of 10 mm^3/5 cm^3, the solutions containing **1** and **2** are saturated, but solutions of **3** and **4** are able to dissolve more $CHCl_3$. Addition of 15 mm^3 of $CHCl_3$ again increases the magnitude of the *Cotton* effects of **3** and **4**, and at this point the solutions become saturated and the *Cotton* effects reach their maximum values (Table 6). The sluggishness of **3** to invert, coupled with the less intense *Cotton* effect of **1** when compared to **2** at $CHCl_3$ saturation, suggests that **1** and **3** are initially more tightly bound to HSA in a favorable binding site than their counterparts. Conversely, rubin

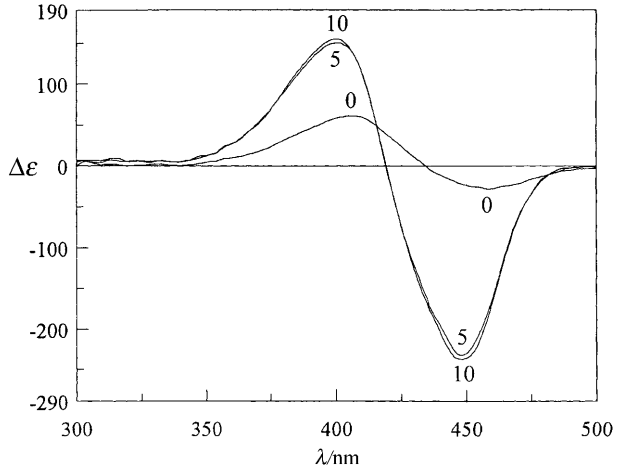

Fig. 7. Circular dichroism spectra of 1.40×10^{-5} *M* **2** in the presence of 2.80×10^{-5} *M* HSA in *pH* 7.4 *Tris* buffer at 22°C upon addition of $CHCl_3$; the amounts of $CHCl_3$ added (mm^3/5 cm^3 buffered pigment-albumin solutions) are indicated on each CD curve (mm^3)

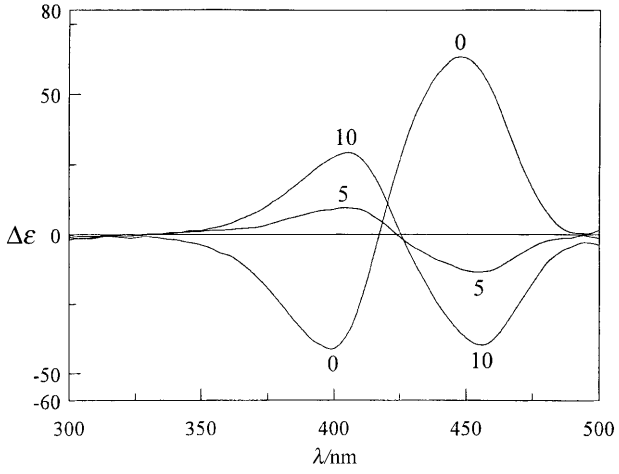

Fig. 8. Circular dichroism spectra of 1.43×10^{-5} *M* **1** in the presence of 2.90×10^{-5} *M* HSA in *pH* 7.4 *Tris* buffer at 22°C upon addition of $CHCl_3$; the amounts of $CHCl_3$ added (mm^3/5 cm^3 buffered pigment-albumin solutions) are indicated on each CD curve (mm^3)

2 initially displays a negative chirality *Cotton* effect and greatly increases in magnitude with increasing amounts of $CHCl_3$. The *Cotton* effects for rubin **4** invert immediately with only a trace of $CHCl_3$, and at the saturation limit the *Cotton* effect is greater than for its counterpart **3**. This suggests that *endo* aromatic and vinyl rubins **2** and **4** are more tightly bound to HSA than their *exo* counterparts after the addition of $CHCl_3$. Apparently, it is the *exo* location of the unsaturated groups rather than their presence that is responsible for the initial favorable binding to HSA, and the *endo* location of these groups that is responsible for favored binding after treatment with $CHCl_3$.

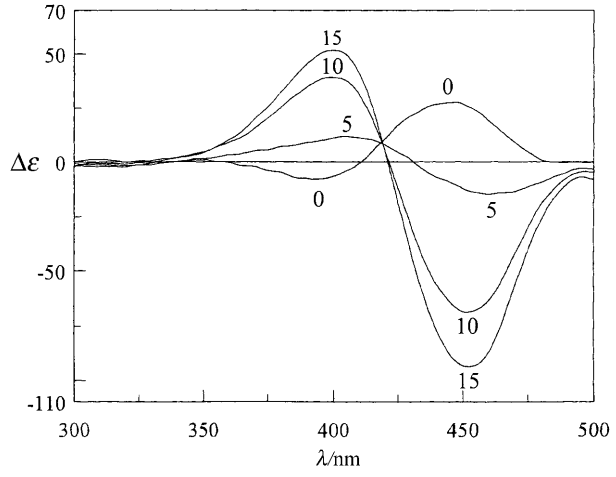

Fig. 9. Circular dichroism spectra of $1.47 \times 10^{-5}\,M$ **4** in the presence of $2.86 \times 10^{-5}\,M$ HSA in *pH* 7.4 *Tris* buffer at 22°C upon addition of $CHCl_3$; the amounts of $CHCl_3$ added (mm^3/5 cm^3 buffered pigment-albumin solutions) are indicated on each CD curve (mm^3)

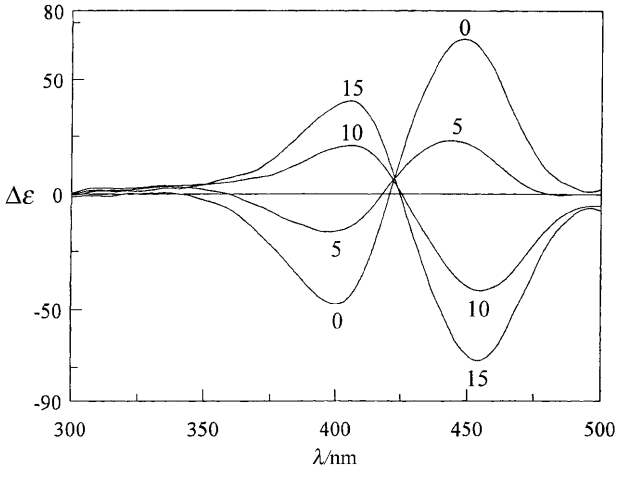

Fig. 10. Circular dichroism spectra of $1.42 \times 10^{-5}\,M$ **3** in the presence of $2.84 \times 10^{-5}\,M$ HSA in *pH* 7.4 *Tris* buffer at 22°C upon addition of $CHCl_3$; the amounts of $CHCl_3$ added (mm^3/5 cm^3 buffered pigment-albumin solutions) are indicated on each CD curve (mm^3)

Concluding comments

In this paper we describe the synthesis and characterization of two new aromatic bilirubin analogs, **1** and **2**. The *exo vs. endo* location of their 2 *o*-fluorophenyl groups might not be expected to play a significant role in the linear (Fig. 1) or porphyrin-like conformations, but in the intramolecularly hydrogen-bonded ridge-tile conformation, the *exo o*-fluorophenyl acts to shield the lactam hydrogen bonding region (Fig. 3). The *endo o*-fluorophenyl is too far away to exert a similar effect. The studies show that introduction of the aromatic groups can have a marked effect on the polarity of the pigments, making **1** and **2** expectedly less polar

Table 6. Influence of $CHCl_3$ on the circular dichroism spectra of **1**–**4**[a] in *pH* 7.4 *Tris* buffer containing HSA

Pigment	$CHCl_3$	CD			UV/Vis	
	(mm^3)	$\Delta\varepsilon^{max}$ $(\lambda)_1$	λ_2 at $\Delta\varepsilon = 0$	$\Delta\varepsilon^{max}$ $(\lambda)_3$	ε^{max}	λ(nm)
1		−41 (400)	417	+63 (447)	43200	452
2	0 mm^3	+60 (406)	434	−29 (459)	52200	454
3		−63 (408)	354	+67 (449)	54470	462
4		−8 (393)	411	+27 (447)	37670	455
1		+9 (404)	424	−14 (454)	41600	449
2	5 mm^3	+149 (400)	419	−233 (448)	62400	452
3		−17 (397)	418	+23 (443)	55570	461
4		+12 (404)	431	−15 (460)	39570	451
1		+29 (406)	426	−40 (456)	44680	452
2	10 mm^3	+154 (400)	419	−238 (448)	62250	452
3		+21 (406)	425	−42 (455)	56520	460
4		+39 (399)	422	−69 (452)	40930	449
1		[b]	[b]	[b]	[b]	[b]
2	15 mm^3	[b]	[b]	[b]	[b]	[b]
3		+40 (406)	425	−72 (454)	58130	460
4		+51 (400)	421	−94 (452)	43830	449

[a] $CHCl_3$ was added to 5 cm^3 solutions that were $\sim 1.4 \times 10^{-5}$ *M* in pigment and had a 1:2 molar ratio of pigment to HSA (human serum albumin) at 22°C; [b] solubility limit of $CHCl_3$ exceeded

(based on HPLC and TLC) than the parent bilirubins (**3** and **4**). The increased lipophilicity has some effect on the CD spectroscopic properties of **1** and **2**, from which one can discern that the presence of an *exo o*-fluorophenyl appears to interfere with complexation to human serum albumin. The energetically most stable conformation of **1** and **2** is still the folded ridge-tile structure preferred by bilirubin and it symmetric analogs, bilirubins **3** and **4**. In preliminary metabolic experiments in rats (carried out by Dr. *A. F. McDonagh* at the University of California, San Francisco), the presence of the *o*-fluorophenyl groups does not appear to prevent rapid uptake of the compound from blood into the liver, but the *exo/endo* location of the aromatic ring seems to affect glucuronidation by bilirubin glucuronosyl transferase. Thus, **2** (with *endo o*-fluorophenyl groups) exhibits less efficient glucuronide formation and excretion than **1**.

Experimental

General

All UV/Vis spectra were recorded on a Perkin-Elmer λ-12 spectrophotometer, and all circular dichroism (CD) spectra on a Jasco J-600 instrument. Nuclear magnetic resonance (NMR) spectra were obtained on a GE QE-300 spectrometer operating at 300 MHz, or on a Varian Unity Plus 500 MHz spectrometer in $CDCl_3$ unless otherwise specified. Chemical shifts are reported in δ/ppm referenced to the residual $CHCl_3$ ^1H signal at 7.26 ppm and the $CHCl_3$ ^{13}C signal at 77.230 ppm. *J*-modulated spin-echo (APT) and HMQC experiments were used to assign ^{13}C NMR spectra. Melting

points were taken on a MelTemp capillary apparatus and are uncorrected. Combustion analyses of the new compounds were carried out by Desert Analytics, Tucson, AZ; the results were within 0.40% of the calculated values. Analytical thin layer chromatography was carried out on J. T. Baker silica gel IB-F plates (125 μ layers). Flash column chromatography was carried out using Woelm silica gel F, thin layer chromatography grade. HPLC analyses were carried out on a Perkin-Elmer Series 4 high performance liquid chromatograph with an LC-95 UV/Vis spectrophotometric detector (410 nm). The column was a Beckman-Altex ultrasphere-IP 5 μm C-18 ODS column (25 $\times$ 0.46 cm) fitted with a similarly-packed precolumn (4.5 $\times$ 0.46 cm). The flow rate was 0.75–1.0 cm^3/minute; the elution solvent was 0.1 *M* di-*n*-octylamine acetate in 5% aqueous MeOH, the column temperature was $\sim$34°C.

Commercial reagents were used as received from Aldrich or Acros, HPLC grade MeOH was from Fisher, human serum albumin (defatted) was obtained from Sigma. Spectroscopic data were obtained in spectral grade solvents (Aldrich or Fisher).

CD and UV measurements

Stock solutions of **1–4** ($\sim 7.0 \times 10^{-4}$ *M*) were prepared by dissolving an appropriate amount of the desired compound in 2 cm^3 of *DMSO*. Next, 100 mm^3 of the stock solution were diluted to 5 cm^3 (volumetric flask) with an HSA solution ($\sim 2.8 \times 10^{-5}$ *M* in *pH* 7.4 *Tris* buffer). The final concentration of the solution was $\sim 1.4 \times 10^{-5}$ *M* in pigment. Up to four 5 cm^3 solutions of each pigment were prepared, as needed, in 5 cm^3 volumetric flasks. To each flask, the indicated volume (mm^3) of $CHCl_3$ was added. Gentle shaking was occasionally required to dissolve all of the $CHCl_3$ in the aqueous solution, at which point CD and UV/Vis measurements were recorded.

5,5′-Diformyl-3,3′-bis-(2-methoxycarbonylethyl)-4,4′-dimethyl-2,2′-dipyrrylmethane (**16**)

16 was prepared according to a literature procedure [12].

1-(o-Fluorophenyl)-2-nitro-1-propanol ($C_9H_8N_{11}O_4F_2$)

o-Fluorobenzaldehyde (116.00 g, 0.93 mol) and KF (2.7 g, 0.05 mol eq.) was stirred mechanically with 400 cm^3 of 2-propanol while a solution of nitroethane (71.00 g, 0.93 mol) in 100 cm^3 of 2-propanol was added dropwise with stirring over several hours. Stirring was continued for 2 days at room temperature. The mixture was then diluted with CH_2Cl_2 and washed with H_2O (3 $\times$ 300 cm^3) and brine (300 cm^3). The organic extracts were dried over anhydrous. $MgSO_4$, filtered, and the solvent was removed. The resulting yellow oil was sufficiently pure for the next step.

Yield: 186.1 g (quantitative); IR (neat): $\nu = 3511$, 2993, 1617, 1555, 1490, 1458, 1226, 1053 cm^{-1}; ^{1}H NMR: $\delta = 7.58$–7.03 (4H, m), 5.72–5.39 (2 $\times$ d, 1H), 4.89–4.76 (2 $\times$ dq, 1H), 2.93 (d, J = 3.0 Hz, 1H), 2.80 (d, $J = 3.0$ Hz, 1H), 1.47 (d, $J = 6.0$ Hz, 3H), 1.41 (d, $J = 6.0$ Hz, 3H) ppm; ^{13}C NMR: $\delta = 161.44$, 160.78, 158.18, 157.55, 130.36, 130.26, 129.91, 129.79, 128.22, 128.18, 127.73, 125.92, 125.75, 125.64, 125.47, 124.64, 124.60, 124.32, 124.29, 115.48, 115.19, 114.92, 87.75, 85.44, 69.88, 68.64, 15.48, 11.83 ppm; MS: *m/z* (%) = 152 (31), 125 (100), 109 (19), 97 (56), 77 (39), 51 (27) amu.

1-(o-Fluorophenyl)-2-nitro-propyl acetate (**15**; $C_{11}H_{12}NO_4F$)

1-(*o*-Fluorophenyl)-2-nitro-1-propanol (50.00 g, 0.25 mol) and *DMAP* (200 mg) were dissolved in 150 cm^3 of acetic anhydride and stirred at room temperature overnight. The solution was then chilled in an ice bath, and H_2O (150 cm^3) was added. Stirring was continued for several hours, after which the mixture was diluted with CH_2Cl_2 (200 cm^3) and washed successively with H_2O (2 $\times$ 500 cm^3), aqueous

$NaHCO_3$ solution ($2 \times 500\,cm^3$), and brine ($500\,cm^3$). The organic layer was dried over anhydrous $MgSO_4$, filtered, and the solvent was removed to yield a light green oil.

Yield: 56.83 g (94%); b.p.: ~128°C (0.45 mm Hg); IR (neat): $\nu = 2996$, 1752, 1559, 1457, 1391, 1221 cm^{-1}; ^1H NMR: $\delta = 7.40$–7.06 (m, 4H), 6.62 (d, $J = 5.0$ Hz, 1H), 6.35 (d, $J = 9.0$ Hz, 1H), 5.09–4.90 ($2 \times$ dq, 1H), 2.22 (s, 3H), 2.03 (s, 3H), 1.54 (d, $J = 7.0$ Hz, 3H), 1.41 (d, $J = 7.0$ Hz, 3H) ppm; ^{13}C NMR: $\delta = 168.50$, 168.41, 166.29, 166.14, 161.76, 161.06, 158.42, 157.74, 131.00, 130.90, 130.58, 128.67, 127.75, 124.67, 124.42, 122.79, 122.67, 122.63, 122.60, 122.35, 122.28, 122.25, 122.19, 115.78, 115.60, 115.48, 115.32, 84.80, 83.42, 70.77, 69.43, 21.48, 19.97, 15.48, 12.80 ppm; MS: *m/z* (%) = 241 (6), 194 (20), 152 (100), 135 (60), 109 (25), 57 (9) amu.

3-(o-Fluorophenyl)-4-methyl-2-p-toluenesulfonyl-1H-pyrrole (**12**; $C_{18}H_{16}NO_2F$)

p-Toluenesulfonyl methyl isocyanide (*TosMIC*) (20.00 g, 0.10 mol) and K_2CO_3 (60 g) were partially dissolved in 100 cm^3 of a mixture of *THF*:2-propanol = 1:1 and stirred magnetically at room temperature. A solution of 1-(*o*-fluorophenyl)-2-nitro-propyl acetate (**15**; 20.00 g, 0.08 mol) was added dropwise, and the mixture was stirred at room temperature for 5 days. It was then diluted with 200 cm^3 of CH_2Cl_2, washed with H_2O ($2 \times 200\,cm^3$) and brine ($200\,cm^3$), and dried over $MgSO_4$. The solvent was removed on a rotary evaporator, and the residue was crystallized from CH_2Cl_2/hexane to yield a tan solid. An analytical sample was prepared by recrystallization from CH_2Cl_2/hexane. The colorless crystals were collected and dried overnight in a drying pistol over P_2O_5.

Yield: 14.8 g (54%); m.p.: 168–169°C; IR (KBr): $\nu = 3301$, 1596, 1471, 1213, 1140, 1082, 753 cm^{-1}; ^1H NMR: $\delta = 9.27$ (s, 1H), 7.35–6.98 (m, 8H), 6.81 (d, $J = 2.5$, 1H), 2.34 (s, 3H), 1.87 (s, 3H) ppm; ^{13}C NMR: $\delta = 160.19$ ($J_{CF} = 246$ Hz), 143.65, 139.27, 133.60 ($J_{CF} = 3.3$ Hz), 129.78 ($J_{CF} = 8.8$ Hz), 129.43, 126.91, 125.13, 123.56 ($J_{CF} = 3.3$ Hz), 123.27, 122.19, 120.61, 120.41 ($J_{CF} = 6.8$ Hz), 115.16 ($J_{CF} = 22$ Hz), 21.61, 1033 ($J_{CF} = 2.2$ Hz) ppm.

5-Bromo-2-p-toluenesulfonyl-3-(o-fluorophenyl)-4-methyl-5-bromo-1H-pyrrole
(**14**; $C_{18}H_{15}NO_2SBrF$)

3-(*o*-Fluorophenyl)-4-methyl-2-*p*-toluenesulfonyl-1*H*-pyrrole (**12**; 0.50 g, 1.51 mmol) was dissolved in 10 cm^3 of CH_2Cl_2 and stirred magnetically in an ice bath. A solution of phenyl trimethyl ammonium tribromide (*PTT*) (1.20 g, 2 eq.) in 20 cm^3 of CH_2Cl_2 was added dropwise, and the resulting yellow-orange solution was stirred at 0°C for 30 min. Subsequently, it was washed with aqueous $NaHSO_3$ solution ($2 \times 30\,cm^3$) and brine ($30\,cm^3$) and dried over $MgSO_4$. The solvent was removed using a rotary evaporator to yield a colorless solid (0.54 g, 87%). An analytical sample was prepared by the addition of hexane to a solution of the pyrrole in CH_2Cl_2. Colorless crystals were collected and dried over P_2O_5 in a drying pistol overnight.

Yield: 0.54 g (87%); m.p.: 157–158°C; IR (KBr): $\nu = 3285$, 1596, 1465, 1317, 1240, 1186, 762 cm^{-1}; ^1H NMR: $\delta = 9.23$ (s, 1H), 7.41–6.99 (m, 8H), 2.35 (s, 3H), 1.80 (s, 3H) ppm; ^{13}C NMR: $\delta = 160.15$ ($J_{CF} = 247.2$ Hz), 144.10, 138.76, 133.60 ($J_{CF} = 3.3$ Hz), 130.35 ($J_{CF} = 7.7$ Hz), 129.59, 127.16, 126.34, 123.97, 123.79 ($J_{CF} = 3.3$ Hz), 122.30, 119.76 ($J_{CF} = 16.5$ Hz), 104.61, 21.76, 10.46 ppm; MS: *m/z* (%) = 409 (100), 343 (77), 269 (15), 160 (39), 91 (25) amu.

4-(o-Fluorophenyl)-3-methyl-5-p-toluenesulfonylpyrrolin-2-one (**10**; $C_{18}H_{16}NO_3SF$)

5-Bromo-2-*p*-toluenesulfonyl-3-(*o*-fluorophenyl)-4-methyl-5-bromo-1*H*-pyrrole (**14**; 5.00 g, 12.25 mmol) was dissolved in 45 cm^3 of *TFA* and 8 cm^3 of H_2O and then stirred at room temperature for 2 days. The resulting dark solution was diluted with 50 cm^3 of CH_2Cl_2 and washed sequentially with H_2O ($2 \times 50\,cm^3$), aqueous $NaHCO_3$ solution ($2 \times 50\,cm^3$), and brine ($50\,cm^3$), then dried over

anhydrous $MgSO_4$. The solvent was removed on a rotary evaporator to yield a light grey powder. Colorless crystals were obtained by the addition of hexane to a solution of the pyrrolinone in CH_2Cl_2. They were collected and dried overnight in a drying pistol over P_2O_5.

Yield: 4.18 g (99%); m.p.: 148–150°C; IR (KBr): $\nu = 3419$, 1706, 1490, 1321, 1137, 811, 761 cm^{-1}; ^1H NMR: $\delta = 7.65$ (d, $J = 8$ Hz, 2H), 7.24 (d, $J = 8$ Hz, 2H), 7.43 (br t, 1H), 7.17 (dt, $J = 3$, 3H), 6.82 (br s, 1H), 5.82 (br s, 1H), 2.42 (s, 3H), 1.78 (s, 3H) ppm; ^{13}C NMR: $\delta = 172.81$, 159.92 ($J_{CF} = 250$ Hz), 145.85, 139.78, 136.82, 131.68 ($J_{CF} = 8$ Hz), 131.00, 130.86 ($J_{CF} = 3$ Hz), 129.73, 129.62, 124.30 ($J_{CF} = 3$ Hz), 119.39 ($J_{CF} = 14$ Hz), 116.37 ($J_{CF} = 22$ Hz), 77.75, 21.90, 10.34 ppm.

4-(o-Fluorophenyl)-3-methylpyrrolin-2-one (**8**; $C_{11}H_{10}NOF$)

4-(*o*-Fluorophenyl)-3-methyl-5-*p*-toluenesulfonyl-pyrrolin-2-one (**10**; 0.10 g, 0.29 mmol) and $NaBH_4$ (23.0 mg, 0.60 mmol) were stirred in 10 cm^3 of absolute EtOH at room temperature for 15 min. The solution was then diluted with 15 cm^3 of CH_2Cl_2, washed with H_2O (2×15 cm^3) and brine (15 cm^3), and dried over $MgSO_4$. The solvent was evaporated on a rotary evaporator, and the residue was crystallized from CH_2Cl_2/hexane to afford a light tan powder (55.0 mg, 90%). An analytical sample was prepared by precipitation from a solution in CH_2Cl_2 with hexane. The colorless crystals were collected and dried over P_2O_5 in a drying pistol overnight.

M.p.: 142–143°C; IR (KBr): $\nu = 3210$, 1687, 1490, 1360, 1267, 1236, 124 cm^{-1}; ^1H NMR: $\delta = 8.07$ (br s, 1H), 7.33 (dt, $J = 2$, 7 Hz, 2H), 7.20 (t, $J = 7$ Hz, 1H), 7.14 (t, $J = 7$ Hz, 1H), 4.26 (s, 3H), 1.95 (d, $J_{HF} = 1$ Hz, 3H) ppm; ^{13}C NMR: $\delta = 175.78$, 159.63 ($J_{CF} = 250$ Hz), 144.89, 132.22, 130.55 ($J_{CF} = 22$ Hz), 130.00 ($J_{CF} = 3$ Hz), 124.33 ($J_{CF} = 3$ Hz), 121.68 ($J_{CF} = 14$ Hz), 116.30 ($J_{CF} = 22$ Hz), 49.13 ($J_{CF} = 5$ Hz), 10.16 ppm.

3,17-Desvinyl-3,17-bis-(o-fluorophenyl)bilirubin-XIIIα (**2**; $C_{41}H_{38}N_4O_6F_2$)

In a 50 cm^3 round bottom flask, 4-(*o*-fluorophenyl)-3-methyl-pyrrolin-2-one (**8**; 0.10 g, 0.52 mmol) and diformyl-dipyrrylmethane [12, 30] (42.0 mg, 0.10 mmol) was dissolved in 20 cm^3 of MeOH and 13 cm^3 of 6 *M* aqueous KOH. The solution was heated at reflux for 48 h. The resulting reddish solution was then chilled in an ice bath and poured into 50 cm^3 of ice water. Acidification by slow addition of concentrated HCl yielded a brown precipitate that was collected by centrifugation and filtration. It was dissolved in CH_2Cl_2 and triturated with MeOH to afford a bright yellow precipitate that was collected by filtration.

Yield: 20.3 mg (27%); m.p.: 254–258°C (dec); IR (KBr): $\nu = 3412$, 1685, 1491, 1400, 1251, 1105, 754 cm^{-1}; ^1H NMR: $\delta = 1.86$ (s, 6H), 2.02 (s, 6H), 2.56 (ddd, $J = 2.48$, 3.16, −14.01 Hz, 2H), 2.80 (ddd, $J = 2.74$, 3.16, −16.00 Hz, 2H), 2.89 (ddd, $J = 13.73$, 2.48, −16.00 Hz, 2H), 3.01 (ddd, $J = 13.73, 2.74, -14.01$ Hz, 2H), 4.08 (s, 2H), 5.84 (s, 2H), 7.451−7.192 (m, 8H), 9.26 (s, 2H), 10.98 (s, 2H), 13.59 (s, 2H) ppm; ^{13}C NMR: $\delta = 9.37$, 10.30, 18.77, 22.50, 32.75, 104.13, 116.40, 119.87, 119.88, 124.24, 124.71, 125.04, 126.97, 128.38, 130.83, 131.84, 134.04, 140.21, 160.11, 173.99, 179.85 ppm.

4-(o-Fluorophenyl)-3-methyl-2-p-toluenesulfonyl-1H-pyrrole (**11**; $C_{18}H_{16}NO_2SF$)

3-(*o*-Fluorophenyl)-4-methyl-2-*p*-toluenesulfonyl-1*H*-pyrrole (**12**; 6.0 g, 18.2 mmol) was dissolved in 18 cm^3 of *TFA* and 164 cm^3 of CH_2Cl_2 to make a 0.1 *M* solution. The solution was stirred at room temperature for 4 days, during which time it darkened. It was washed with H_2O (2×200 cm^3), aqueous $NaHCO_3$ solution (2×200 cm^3), and brine (200 cm^3); then it was dried over $MgSO_4$. The solvent was removed on a rotary evaporator and the residue crystallized from CH_2Cl_2/hexane to afford a tan solid. Colorless crystals were obtained by precipitation from CH_2Cl_2/hexane. They were collected and dried overnight in a drying pistol over P_2O_5.

Yield: 5.54 g (92%); m.p.: 158–159°C; IR (KBr): $\nu = 3366$, 1315, 1229, 1188, 1086, 814 cm^{-1}; ^1H NMR: $\delta = 9.25$ (br s, 1H), 7.82 (d, $J = 8.4$ Hz, 2H), 7.31 (d, $J = 8.4$ Hz, 2H), 7.27−7.02 (m, 4H),

7.04 (d, $J = 2$ Hz, 1H), 2.42 (s, 3H), 2.22 (d, $J_{HF} = 1$ Hz, 3H) ppm; ^{13}C NMR: $\delta = 159.91$ ($J_{CF} = 246$ Hz), 143.93, 139.66, 131.46 ($J_{CF} = 3.3$ Hz), 129.97, 129.66 ($J_{CF} = 8.8$ Hz), 126.81, 124.61, 124.51, 124.05 ($J_{CF} = 3.3$ Hz), 122.54, 121.98 ($J_{CF} = 15.4$ Hz), 120.97, 115.83 ($J_{CF} = 23$ Hz), 21.68, 10.41 ($J_{CF} = 3.3$ Hz) ppm.

5-Bromo-4-(o-fluorophenyl)-3-methyl-2-p-toluenesulfonyl-1H-pyrrole (**13**; $C_{18}H_{18}NO_2SBrF$)

Compound **13** was prepared as described for 5-bromo-2-*p*-toluenesulfonyl-3-(*o*-fluorophenyl)-4-methyl-5-bromo-1*H*-pyrrole (**14**) using 5.69 g (17.3 mmol) of 2-(*p*-tosyl)-3-methyl-4-(*o*-fluorophenyl)-1*H*-pyrrole and 13.0 g (2.0 eq.) of *PTT*.

Yield: 6.85 g (97%); m.p.: 140–141°C; IR (KBr): $\nu = 3287$, 1464, 1232, 1183, 1067, 817 cm^{-1}; ^{1}H NMR: $\delta = 9.64$ (br s, 1H), 7.85 (d, $J = 8$ Hz, 2H), 7.33 (d, $J = 8$ Hz, 2H), 7.20−7.09 (m, 4H), 2.43 (s, 3H), 2.14 (s, 3H) ppm; ^{13}C NMR: $\delta = 160.26$ ($J_{CF} = 249$ Hz), 144.22, 139.472, 132.66 ($J_{CF} = 2.2$ Hz), 130.07, 129.92 ($J_{CF} = 8.8$ Hz), 127.01, 126.61, 125.76, 124.07 ($J_{CF} = 3.3$ Hz), 121.70, 120.35 ($J_{CF} = 15.4$ Hz), 115.92 ($J_{CF} = 22$ Hz), 105.89, 21.71, 10.56 ($J_{CF} = 2.2$ Hz) ppm; MS: *m/z* (%) = 409 (100), 344 (15), 188 (45), 172 (96), 133 (81), 91 (24) amu.

3-(o-Fluorophenyl)-4-methyl-5-p-toluenesulfonyl-pyrrolin-2-one (**9**; $C_{18}H_{16}NO_3SF$)

Compound **9** was prepared as described for 4-(*o*-fluorophenyl)-3-methyl-5-*p*-toluenesulfonyl-pyrrolin-2-one (**10**) using 2.00 g (4.90 mmol) of 5-bromo-4-(*o*-fluorophenyl)-3-methyl-2-*p*-toluenesulfonyl-1*H*-pyrrole (**13**).

Yield: 1.45 g (86%); m.p.: 188–189°C; IR (KBr): $\nu = 3426$, 1700, 1496, 1387, 1318, 1207, 1137, 1080, 819, 760, 630, 588 cm^{-1}; ^{1}H NMR: $\delta = 7.72$ (d, $J = 8$ Hz, 2H), 7.31 (d, $J = 8$ Hz, 2H), 7.14−6.96 (m, 4H), 6.86 (s, 1H), 5.21 (br s, 1H), 2.40 (s, 3H), 2.24 (d, $J_{HF} = 2.2$ Hz, 3H) ppm; ^{13}C NMR: $\delta = 171.1$, 159.81 ($J_{CF} = 250$ Hz), 147.80, 146.30, 132.01, 131.15 ($J_{CF} = 3.3$ Hz), 130.87 ($J_{CF} = 8.8$ Hz), 130.05, 129.88, 129.79, 124.15 ($J_{CF} = 3.3$ Hz), 117.54 ($J_{CF} = 15.4$ Hz), 115.95 ($J_{CF} = 22$ Hz), 79.54, 21.92, 14.99 ($J_{CF} = 4.4$ Hz) ppm.

3-(o-Fluorophenyl)-4-methyl-pyrrolin-2-one (**7**; $C_{11}H_{10}NOF$)

Compound **7** was prepared as described for 4-(*o*-fluorophenyl)-3-methyl-pyrrolin-2-one (**8**) using 1.00 g (2.90 mmol) of 3-(*o*-fluorophenyl)-4-methyl-5-*p*-toluenesulfonyl-pyrrolin-2-one (**9**) and 0.23 g (2 eq.) of $NaBH_4$.

Yield: 0.54 g (98%); m.p.: 158–159°C; IR (KBr): $\nu = 3198$, 1678, 1660, 1490, 1456, 1211, 755, 688 cm^{-1}; ^{1}H NMR: $\delta = 7.74$ (br s, 1H), 7.41−7.09 (m, 4H), 4.01 (br s, 2H), 2.04 (s, 3H) ppm; ^{13}C NMR: $\delta = 174.54$, 160.08 ($J_{CF} = 250$ Hz), 154.54, 131.65 ($J_{CF} = 3$ Hz), 129.95 ($J_{CF} = 9$ Hz), 127.65, 124.17 ($J_{CF} = 3$ Hz), 119.27 ($J_{CF} = 15$ Hz), 115.88 ($J_{CF} = 22$ Hz), 50.93, 14.82 ($J_{CF} = 3$ Hz) ppm.

2,18-Desvinyl-2,18-bis-(o-fluorophenyl)bilirubin-IIIα (**1**; $C_{41}H_{38}N_4O_6F_2$)

Compound **1** was prepared exactly as described for 3,17-desvinyl-3,17-*bis*-(*o*-fluorophenyl)-bilirubin-XIIIα (**2**).

Yield: 44.3 mg (59%); m.p.: 275–280°C (dec); IR (KBr): $\nu = 3417$, 2924, 1685, 1617, 1498, 1399, 1248, 778 cm^{-1}; ^{1}H NMR: $\delta = 2.14$ (d, $J_{HF} = 2.10$ Hz, 6H), 2.20 (s, 6H), 2.60 (ddd, $J = 2.74$, 3.20, −13.23 Hz, 2H), 2.82 (ddd, $J = 2.74$, 3.20, −18.48 Hz, 2H), 2.92 (ddd, $J = 13.81$, 2.74, −18.48 Hz, 2H), 3.04 (ddd, $J = 13.81$, 3.20, −13.23 Hz, 2H), 4.11 (s, 2H), 6.26 (s, 2H), 7.12 (m, 2H), 7.19 (m, 2H), 7.31 (m, 2H), 7.37 (m, 2H), 9.36 (s, 2H), 10.88 (s, 2H), 13.53 (s, 2H) ppm; ^{13}C NMR: $\delta = 10.43$, 11.27, 18.80, 22.55, 32.78, 102.86, 116.10, 119.39, 120.09, 122.32, 124.26, 124.60, 125.38, 129.26, 129.97, 131.92, 134.32, 145.61, 160.15, 172.99, 179.87 ppm.

Acknowledgments

We thank the National Institutes of Health (HD-17779) for support of this research.

References

[1] McDonagh AF (1975) In: Dolphin D (ed) The Porphyrins, vol 6. Academic Press, New York, p 293
[2] Chowdhury JR, Wolkoff AW, Chowdhury NR, Arias IM (1995) Hereditary Jaundice and Disorders of Bilirubin Metabolism. In: Scriver CR, Beaudet AL, Sly WS, Valle D (eds) The Metabolic and Molecular Bases of Inherited Disease, vol II. McGraw-Hill, New York, p 2161
[3] Bonnett R, Davies JE, Hursthouse MB, Sheldrick GM (1978) Proc R Soc London Ser B **202**: 249
[4] Person RV, Peterson BR, Lightner DA (1994) J Am Chem Soc **116**: 42
[5] Nogales DF, Ma JS, Lightner DA (1993) Tetrahedron **49**: 2361
[6] Boiadjiev SE, Anstine DT, Lightner DA (1995) J Am Chem Soc **117**: 8727
[7] Chen Q, Lightner DA (1998) J Org Chem **63**: 2665
[8] Huggins MT, Lightner DA (2000) J Org Chem **65**: 6001
[9] McDonagh AF, Lightner DA (1991) In: Bock KW, Gerok W, Matern S (eds) Hepatic Metabolism and Disposition of Endo and Xenobiotics (Falk Symposium No 57). Kluwer, Dordrecht, chap 5, p 47
[10] Trull FR, Franklin RW, Lightner DA (1987) J Heterocyclic Chem **24**: 1573
[11] Brower JO, Lightner DA, McDonagh AF (2000) Tetrahedron **56**: 7869
[12] Chen Q, Huggins MT, Lightner DA, Norona W, McDonagh AF (1999) J Am Chem Soc **121**: 9253
[13] Barton DHR, Kervagoret J, Zard SZ (1990) Tetrahedron **46**: 7587
[14] Kohori K, Kinoshita H, Inomata K (1995) Chem Lett 799
[15] Fischer H, Orth H (1937) Die Chemie des Pyrrols, vol II, first half. Akademische Verlagsgesellschaft, Leipzig
[16] Dörner T, Knipp B, Lightner DA (1997) Tetrahedron **53**: 2697
[17] Navon G, Frank S, Kaplan D (1984) J Chem Soc Perkin Trans 2, 1145
[18] Trull FR, Ma JS, Landen GL, Lightner DA (1983) Israel J Chem **23**: 211
[19] Gawroński JK, Połonski T, Lightner DA (1990) Tetrahedron **46**: 8053
[20] Falk H (1989) The Chemistry of Linear Oligopyrroles and Bile Pigments. Springer, Wien
[21] Trull FR, Shrout DP, Lightner DA (1992) Tetrahedron **48**: 8189
[22] For leading references, see Kaplan D, Navon G (1983) Israel J Chem **23**: 177
[23] Boiadjiev SE, Lightner DA (1999) Tetrahedron Asymm **10**: 2535
[24] Lightner DA, Gawroński J, Wijekoon WMD (1987) J Am Chem Soc **109**: 6354
[25] Bauman D, Killet C, Boiadjiev SE, Lightner DA, Schönhofer A, Kuball H-G (1996) J Phys Chem **100**: 11546
[26] Harada N, Nakanishi K (1983) Circular Dichroic Spectroscopy – Exciton Coupling in Organic Stereochemistry. University Science Books, Mill Valley, CA
[27] Lightner DA, Wijekoon WMD, Zhang M-H (1988) J Biol Chem **263**: 16669
[28] Lightner DA, An JY, Pu YM (1988) Arch Biochem Biophys **262**: 543
[29] Pu Y-M, McDonagh AF, Lightner DA (1993) J Am Chem Soc **115**: 377
[30] Clezy PS, Fookes CJR, Liepa AJ (1972) Austral J Chem **25**: 1979

Received May 22, 2001. Accepted May 29, 2001